THE JOURNAL OF PHYSICAL CHEMISTRY B
A JOURNAL OF THE AMERICAN CHEMICAL SOCIETY

pubs.acs.org/JPCB

Perspective

Understanding Carotenoid Dynamics via the Vibronic Energy Relaxation Approach

Václav Šebelík,[⊥] Christopher D. P. Duffy,[⊥] Erika Keil, Tomáš Polívka, and Jürgen Hauer*

Cite This: *J. Phys. Chem. B* 2022, 126, 3985−3994

Read Online

ACCESS | Metrics & More | Article Recommendations

ABSTRACT: Carotenoids are an integral part of natural photosynthetic complexes, with tasks ranging from light harvesting to photoprotection. Their underlying energy deactivation network of optically dark and bright excited states is extremely efficient: after excitation of light with up to 2.5 eV of photon energy, the system relaxes back to ground state on a time scale of a few picoseconds. In this article, we summarize how a model based on the vibrational energy relaxation approach (VERA) explains the main characteristics of relaxation dynamics after one-photon excitation with special emphasis on the so-called S* state. Lineshapes after two-photon excitation are beyond the current model of VERA. We outline this future line of research in our article. In terms of experimental method development, we discuss which techniques are needed to better describe energy dissipation effects in carotenoids and within the first solvation shell.

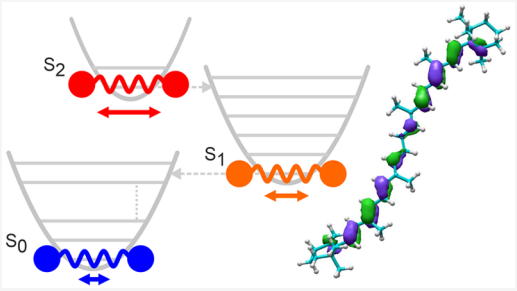

INTRODUCTION

Carotenoids are natural pigments known for their multiple functions in nature, ranging from light-harvesting and photoprotection in photosynthesis to coloration of flowers and animals. The large variety of functions is related to their specific spectroscopic properties related to the presence of dark excites states, which have been a subject of numerous theoretical and experimental studies. These unique excited state properties lead to carotenoid excited lifetimes much shorter than in other biologically relevant pigments such as chlorophylls. The lifetime of the lowest excited state (S_1) of carotenoids shortens with increasing conjugation length, N. For the longest natural carotenoids, the S_1 lifetime drops to 1 ps,[1] and for extremely long synthetic ones, it further decreases to less than 500 fs.[2,3] For long carotenoids, this means that 17500−19500 cm^{-1} of excitation energy—associated with the strongly allowed S_0−S_2 transition in Figure 1a—are transferred to molecular vibrations on the electronic ground state within less than 1 ps. Such ultrafast deactivation must result in pronounced heat dissipation, i.e., a temperature jump in the local solvent environment of the carotenoid. Whether such local heating may have biological relevance remains unknown.

In this article, we aim to present a brief overview of a model to describe vibrational energy relaxation on electronic excited- and ground-state in carotenoids from first principles. The so-called S*-state will serve as a test case for our vibrational energy relaxation approach (VERA). We will sketch the underlying theoretical model and describe how solvent relaxation dynamics can be incorporated. By comparing excited state signatures of S_1 after one- and two-photon excitation, we demonstrate the importance of such solvent-related heat dissipation effects and describe possible future research directions.

THE S* STATE

The history of studies of heat dissipation in carotenoids is closely connected with the yet-elusive spectral feature denoted as the S* state. In transient absorption spectra, the S* signal is readily identified via its characteristic excited-state absorption, squeezed between the ground state bleaching and the main carotenoid ESA band due to the S_1−S_n transition (Figure 1b).[4] This signal was first described in 1995 and assigned to a carotenoid hot ground state.[3] Then, in 2001, it was identified in a light harvesting complex and assigned to a separate excited state denoted S*.[5] In 2004, the hot ground state hypothesis was revived[6] and since then a few different explanations of the S* signal origin were proposed. In the following, we will give a brief overview on the different models proposed to explain the S*-feature.

The Sequential Hot S_0-Model. In general, S* manifests as a shoulder on the S_1−S_n transition. Such a feature is clearly visible already in early ultrafast data on carotenoids,[7] but its importance was first realized in an ultrafast transient absorption study of a very long ($N \approx 18$) derivative of β-carotene.[3] The S* signal

Received: February 10, 2022
Revised: May 3, 2022
Published: May 24, 2022

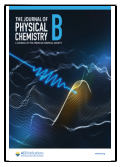

https://doi.org/10.1021/acs.jpcb.2c00996
J. Phys. Chem. B 2022, 126, 3985−3994

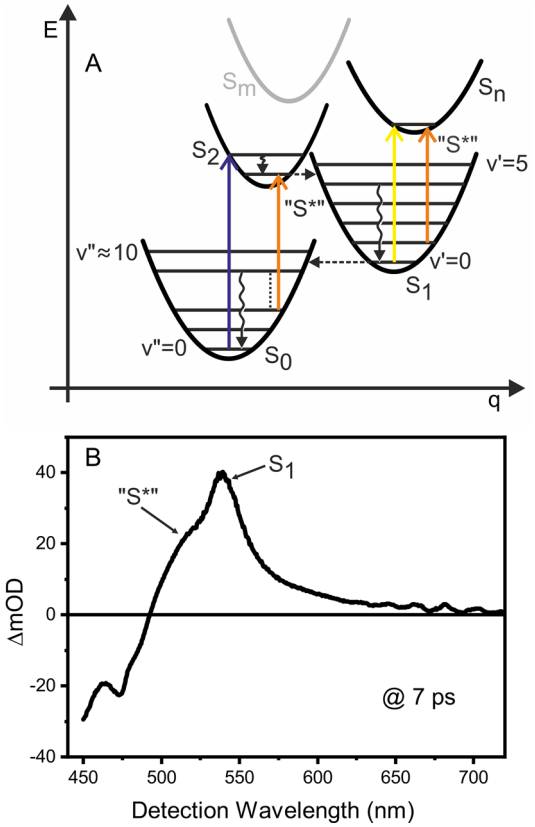

Figure 1. (A) Energy level scheme for carotenoids. Electronic states S_0, S_1, and S_2 are drawn as parabolas. Higher lying states S_n (S_m) explain the ESA-signals from S_1 (and S_2). Vibrational levels, which are an explicit part of the model within VERA, are drawn as horizontal lines. Colored arrows denote optical transitions. The orange arrows indicate the origin of the debate S*-signal, which is here explained as transitions of vibrational nonequilibrium states on both S_1 and S_0. (B) Transient absorption spectrum of lutein in acetone at 7 ps delay time. The main excited state absorption features for S_1 and S* are indicated.

decayed with lifetime longer than the S_1 state, clearly pointing to an origin of the S* signal different from the S_1 state. Due to the spectral position of the S* signal, it was assigned to a hot ground state, leading to a sequence $S_2 \rightarrow$ hot $S_1 \rightarrow S_1 \rightarrow$ hot S_0 (=S*) $\rightarrow S_0$.

The Instantaneous Hot S_0 Model. The above assignment of S* as a sequentially populated hot ground state was later challenged in a study demonstrating that the S* signal of the carotenoid spirilloxanthin bound to a light harvesting complex serves as a precursor for triplet state formation and therefore cannot be a hot ground state based on energetic arguments.[5] The sequential hot S_0-model for S* was further questioned in carotenoids with $N \approx 10-11$, such as the prototypical β-carotene, in which the S* shoulder decayed along with the S_1 state. In these carotenoids, the S* shoulder appears in transient spectra measured at delay times much shorter than the S_1 lifetime, which speaks against the assignment to a hot ground state populated via the internal conversion sequence denoted above. In a separate study,[6] it was suggested that in such a case the hot ground state could be populated directly from S_2 via impulsive Raman scattering. This approach explains the appearance of the S* signal at very early times after excitation. However, this mechanism of populating a hot ground state was ruled out in an experiment using spectrally narrow excitation pulses, which showed identical S*-signatures. A narrowband pulse should not populate a hot ground state via impulse Raman scattering as it lacks the necessary Stokes-shifted components.[8]

S* as a Separate Electronic Excited State and the Inhomogeneous Ground State Model. The apparent lack of a consistent picture for S* instigated several studies attributing S* to a separate electronic excited state. In these studies, the S* state is usually associated with a distinct minimum on the S_1 potential surface, corresponding to a "distorted" S_1 state[9−12] populated directly from the initially excited S_2 state. Such excited state branching however does not explain reported temperature dependences of the S_1/S* ratio.[13] This observation called for a distribution of conformers already on the electronic ground state, as suggested in a quantum mechanical model by Lukeš et al.[14] and previously by Papagianakis et al.[12] based on global fitting of experimental transient absorption data. Briefly, the inhomogeneous ground state model explains S* as the lowest singlet excited state (*i.e.*, S_1) of a symmetric, but nonequilibrium ground state conformer. The energy difference between this symmetric minimum and the (asymmetric) global minimum structure is small: the S*-producing conformer carries 30% of the population at room temperature in the case of β-carotene. Using femtosecond stimulated Raman spectroscopy, Kloz et al.[15] discussed the ultrafast dynamics of high-frequency modes, characteristic to carotenoid first excited states. The fact that two such modes were found that were attributable to S_1 and S* lifetimes in spirilloxanthin added further proof to the excited state character of S* and furthermore to the inhomogeneous ground state model.

S* as a Consequence of Vibrational Cooling on S_1 and S_0. The inhomogeneous ground state model sketched above explains the experimental observations, but leaves the question unanswered as to how a minute change in molecular geometry can lead to drastic lifetime differences as measured for S_1 and S*. A number of studies provided evidence that for carotenoids with $N \geq 12$, the S* lifetime is always distinctively longer than the S_1 lifetime,[2,3,5,16,17] while for shorter ones the S* signal decays with the same lifetime as the S_1 state,[6,18,19] which makes a clear assignment by global (target) analysis challenging. This distinction between early and late contributions to S* provided the basis for kinetic modeling that showed that the S* signal indeed could be captured by a combination of contributions from a (sequentially populated) hot ground state and the S_1 state.[18,20,21] While these studies used a phenomenological fit, in the sense that there was no molecular basis for the employed species, Balevičius et al. showed that a simple—but carefully parametrized—displaced harmonic oscillator model with proper inclusion of vibrational levels of both S_0 and S_1 states can successfully reproduce the S* dynamics.[22] The dynamic model of the S* signal was further elaborated by a more sophisticated model called the vibrational energy redistribution approach (VERA). It was shown that for carotenoids with $N \leq 11$ (such as, *e.g.*, β-carotene), the dominating contribution to the S* signal comes from the S_1 state, but with increasing conjugation, the sequentially populated hot ground state contribution prevails, as the S_1 lifetime becomes shorter than vibrational relaxation in the ground state.[23,24] Such explanation of the S* origin thus accommodates assignment of the S* signal to an excited state as well as to a hot ground state, validating both originally competing hypotheses.

We note, however, that while our approach described here focuses solely on the S* signal reported for carotenoids in solution, there is a number of reports identifying the S* signal in carotenoids bound to proteins. The term "S* state" was coined

https://doi.org/10.1021/acs.jpcb.2c00996
J. Phys. Chem. B 2022, 126, 3985−3994

for the carotenoid spirilloxanthin in purple bacterial antenna complex LH1 where S* was proposed to be a precursor of ultrafast singlet fission forming a triplet state.[5] The S* state was also reported as energy donor in carotenoid-BChl energy transfer in LH2[16,25] or artificial carotenoid-porphyrin dyads,[26] but also as energy acceptor (quencher) in LHCII[27,28] and CP29 complex of plants.[29] In the photoactive orange carotenoid protein (OCP) from cyanobacteria, the S* was proposed to initiate the photocycle.[30] It is thus possible that in these pigment−protein complexes there is not a single origin of the S* signal, but it may originate from multiple phenomena instead. This was demonstrated for example in LH2 complex from purple bacteria, for which the substantial part of the S* signal could be explained by an electrochromic shift of the carotenoid S_2 state.[31]

Here, we will focus on the S* signal in carotenoids in solution. In the following, we want to give a brief overview of the theoretical framework behind VERA. This will be a starting point to explain the model and its future perspectives, especially with respect to incorporation of solvent-related effects.

MODELING THE RELAXATION DYNAMICS OF CAROTENOIDS

Understanding carotenoid electronic structure and relaxation dynamics is a considerable theoretical challenge. Quantum chemical calculations that attempt to derive properties from first-principles are facing the considerable problem of accounting for the strong electron correlations and vibronic couplings that characterize the low-lying excited states.[32−36] This is a large and highly active field of study and will not be discussed in any detail here (for a very recent reappraisal of the subject the reader is directed to Bondanza et al.[37]). Briefly, theory predicts the S_0, S_1, S_2 singlet electronic levels which are related to the canonical $1^1A_g^-$, $2^1A_g^-$, and $1^1B_u^+$ states from π-electron models of linear polyenes.[32] S_1 is a "dark" state since it is a multielectron excitation and therefore possesses a vanishing oscillator strength, an argument that is independent of the inversion symmetry (or lack thereof) of the carotenoid under investigation. Some calculations, particularly on longer carotenoids, predict additional dark states between S_1 and S_2 which may be related to either the $1^1B_u^+$ or $3^1A_g^-$ state.[38] These multiple challenges in electronic structure calculations of even moderately sized carotenoids such as β-carotene ($C_{40}H_{56}$) explain the lack of quantum dynamical simulations for such systems. Therefore, phenomenological models are the most common approach for understanding transient absorption spectra of carotenoids.

Phenomenological models vary in physical detail from essentially none, in the case of global analysis, to being constructed on quantum chemical arguments but treating key quantities as fitting parameters. An example of the latter is the five-state diagrammatic perturbation model of Sugisaki and co-workers,[39−41] used to model degenerate four wave mixing (FWM) measurements on β-carotene[39] (and later a longer homologue[40]). The model was based on three states, S_0, S_1 and S_2, plus higher levels, S_n and S_m, to account for the S_1 and S_2 excited state absorption (ESA) respectively. The excitation energy dependence of the transient grating (TG) signal could only be explained by a dark state, S_X, between S_2 and S_1.[41] The high-frequency wavepacket modulation from C═C, C−C, and $-CH_3$ vibrations, which were clearly visible in the TG, were included as under-damped modes in the bath spectral density. However, they were not included in the description of the population interconversion (IC) between electronic levels, which instead were assigned single decay rate constant (Γ_{12}, Γ_{01}, *etc.*). This approach bears the assumption that vibrational population relaxation on an electronic state is much faster than IC between levels. However, when considering transient measurements covering the full $S_2 \rightarrow S_1 \rightarrow S_0$ relaxation, neglecting vibrational relaxation can prove problematic. In particular, a description of the S*-signal, which was repeatedly attributed to vibrationally excited states as described above,[42] calls for an explicit treatment of vibrational modes as part of the (quantum mechanical) system, rather than vibrations as part of the spectral density. In other words: the idea of *hot* states implied that one must consider the effect of the high frequency modes not just on the optical response functions, but in the relaxation kinetics. The essential feature of VERA to transient absorption (TA), developed by Balevičius and co-workers,[22−24,43] is that it fully quantizes the optically coupled modes meaning that the small number of electronic levels are replaced by a much larger set of *vibronic states*,

$$|i_a\rangle = |i\rangle, \prod_\alpha |a_\alpha^i\rangle \tag{1}$$

where $|i\rangle \equiv |S_i\rangle$ is a pure electronic state and $|a_\alpha^i\rangle$ is a vibrational state of a particular optically coupled mode, α, on $|i\rangle$. The modes assumed to be harmonic, $a_\alpha^i = 0, 1, ..., \infty$ is the vibrational quantum number of mode α, and the index $a = (a_1, a_2, ..., a_{N_\alpha})$ is a tuple of these numbers. It is generally assumed that there are two such modes corresponding to the symmetric C═C and C−C stretching modes. $\{|i_a\rangle\}$ are eigenstates of the vibronic (system) Hamiltonian,

$$H_S = \sum_{i,a} |i_a\rangle\langle i_a| \left(\hbar\omega_i + \sum_a \left(a_\alpha^i + \frac{1}{2} \right) \hbar\omega_\alpha^i \right) \tag{2}$$

where ω_i and ω_α^i are the electronic and vibrational frequencies, respectively. For simplicity it is assumed that $\omega_{C-C} = 1150\ cm^{-1}$ and $\omega_{C=C} = 1520\ cm^{-1}$ regardless of the electronic state (i.e., no Duschinsky rotations). The *bath* consists of the nonoptical vibrational modes, rotation/libration modes, and all solvent degrees of freedom, and it is abstracted as an infinite set of classical harmonic oscillators,

$$H_B = \sum_\kappa \left(\frac{p_\kappa^{\,2}}{2m_\kappa} + \frac{m_\kappa \omega_\kappa^{\,2} x_\kappa^{\,2}}{2} \right) \tag{3}$$

These are assumed to couple to the system in two ways. Some couple adjacent vibrational levels of the same mode on a given electronic state and are therefore responsible for vibrational relaxation on electronic states

$$H_{SB}^{IVR} = \sum_{i,\alpha,\kappa} c_{i\kappa} x_\kappa \sqrt{a_\alpha^i + 1}\, (|i_a\rangle\langle i_{a_\alpha+1}| + |i_{a_\alpha+1}\rangle\langle i_a|) \tag{4}$$

where $|i_{a_\alpha+1}\rangle = |i\rangle\, |a_1^i\rangle\, |a_2^i\rangle \cdots |a_\alpha^i + 1\rangle \cdots |a_{N\alpha}^i\rangle$. For large molecules in solution, the relaxation occurs into the other, nonoptical modes, and therefore, H_{SB}^{IVR} is responsible for intramolecular vibrational redistribution (IVR). Other bath modes couple vibronic states on different electronic levels and are therefore responsible for IC,

https://doi.org/10.1021/acs.jpcb.2c00996
J. Phys. Chem. B 2022, 126, 3985−3994

$$H_{SB}^{IC} = \sum_{i,\kappa,a,b} f_{i\kappa} x_\kappa \left[\left(\prod_\alpha F_{i_a,i+1_b}^\alpha \right) |i_a\rangle\langle i+1_b| + \left(\prod_\alpha F_{i+1_a,i_b}^\alpha \right) |i+1_b\rangle\langle i_a| \right] \quad (5)$$

where $F_{i_{a,j}b}^\alpha = \langle a_\alpha^i | b_\alpha^j \rangle$ are the nuclear wave function overlaps. The equations of motion for the vibronic populations, $n_a^i(t)$, are obtained by treating $H_{SB} = H_{SB}^{IVR} + H_{SB}^{IC}$ as a second-order perturbation,

$$\frac{\mathrm{d}}{\mathrm{d}t} n_a^i = \left(\frac{\mathrm{d}}{\mathrm{d}t} n_a^i \right)_{IVR} + \left(\frac{\mathrm{d}}{\mathrm{d}t} n_a^i \right)_{IC} + \left(\frac{\mathrm{d}}{\mathrm{d}t} n_a^i \right)_{pump} \quad (6)$$

where the final term simulates the initial optical pumping of S_2. The functional forms of the IVR and IC terms are published elsewhere[22,23,43] and are defined by a set of first-order rate constant which, within the framework of secular Redfield theory, are given by Fourier transform of bath correlation function, $C(\omega)$, evaluated at the appropriate energy gap. The rates for the converse vibrational transitions $|i_a\rangle \rightleftharpoons |i_{a_\alpha+1}\rangle$ are

$$k_{a_\alpha+1\leftarrow a_\alpha}^i = (a_\alpha + 1) C_{IVR}(-\omega_\alpha^i) \quad (7)$$

$$k_{a_\alpha\leftarrow a_\alpha+1}^i = a_\alpha C_{IVR}(\omega_\alpha^i) \quad (8)$$

where the *upward* transition, $k_{a_\alpha+1\leftarrow a_\alpha}^i$, is thermally penalized. Similarly, the rates for the converse IC transitions $|i_a\rangle \rightleftharpoons |i+1_b\rangle$ are

$$k_{ba}^{i+1\leftarrow i} = \left(\prod_\alpha |F_{i_a,i+1_b}^\alpha|^2 \right) C_{IC}(-\Delta_{ba}^{i+1,i}) \quad (9)$$

$$k_{ab}^{i\leftarrow i+1} = \left(\prod_\alpha |F_{i_a,i+1_b}^\alpha|^2 \right) C_{IC}(\Delta_{ba}^{i+1,i}) \quad (10)$$

where $\Delta_{ba}^{i+1,i}$ is the vibronic energy gap,

$$\Delta_{ba}^{i+1,i} = (\omega_{i+1} - \omega_i) + \sum_\alpha \left[\omega_\alpha^{i+1} \left(b_\alpha + \frac{1}{2} \right) - \omega_\alpha^i \left(a_\alpha + \frac{1}{2} \right) \right] \quad (11)$$

The correlation functions are related to associated spectral density functions via the fluctuation−dissipation theorem,

$$C_X(\omega) = C_X''(\omega) \left(\coth\left(\frac{\hbar\omega}{2k_B T} \right) + 1 \right) \quad (12)$$

An overdamped Brownian oscillator (Drude model) is assumed for $C_X''(\omega)$, which are therefore characterized by a reorganization energy, λ_α^i or λ_{ij}, and a damping frequency, γ_α^i or γ_{ij}. Finally, the TA spectrum itself is expressed as a combination of ESA, GSB and stimulated emissions (SE) components

$$A(\omega, t) = A_{ESA}(\omega, t) - A_{GSB}(\omega, t) - A_{SE}(\omega, t) \quad (13)$$

The spectral components are decomposed according to,

$$A_X(\omega, t) = \sum_{\substack{ij \\ ab}} n_a^i(t) I_{ab,X}^{ij}(\omega) \quad (14)$$

where $I_{ab,X}^{ij}(\omega)$ is a Franck−Condon weighted Gaussian/Lorentzian line shape functions for a particular vibronic transition. They are centered on energy gap Δ_{ab}^{ij} and have a phenomenological width $\Delta\omega$. All together this yields a model with a very large number of free parameters, although some of these can be constrained via independent measurement or reasonable approximation.

The initial formulation of the VERA was simpler than the general model summarized above, treated only S_1 and S_2 as explicitly vibronic and was applied to β-carotene and a chemical derivative (7-apo-7-(4-aminophenyl)-β-carotene).[22] For β-carotene, it fully reproduced all spectral dynamics. The progressive narrowing and blue shift of the ESA was found to originate from vibrational relaxation on S_1, while the S* shoulder is just that, a vibronic shoulder due to a large S_1−S_n displacement (see Figure 1a). For the derivative, the S* shoulder decays on a different time scale with respect to S_1 and could not be reproduced by the model without the addition of an *ad hoc* inhomogeneous ground state. Later, the model was generalized via the addition of an explicitly vibronic S_0, giving a unified picture of S* as a combination of vibronic features on S_1 and a slow vibrational relaxation on S_0.[23] In the latter case, absorption from an excited vibrational level on the electronic ground state S_0 as shown in Figure 1a leads to a positive, red-shifted peak that happens to coincide with the vibronic shoulder of S_1. Later still, the model was shown to explain the dependence of ESA width on excitation wavelength.[43]

Finally, in 2019 VERA was expanded to a more realistic description of vibrational energy flow between the carotenoid and the solvent.[24] The motivation for this was to attempt to explain the physical origin of the slow IVR on S_0 that gives rise to S*, something that was previously fit by simply assuming very small reorganization energies, λ_α^0. The initial hypothesis was that the slow IVR could be explained by transient local heating. Given that carotenoids are capable of dissipating ~20 000 cm^{-1} of energy in around 2−20 ps, the assumption of an infinite and infinitely fast bath may not be reasonable. The immediate destination of the energy lost during IC and IVR will (largely) be the carotenoids own low frequency, nonoptical vibrational modes, giving a relatively small number of degrees of freedom. From there it will be transferred to the first solvation shell (FSS) and eventually into the solvent bulk. This will not happen instantly, and the transient accumulation of energy in local degrees of freedom may even feed back into the relaxation dynamics of the vibronic subsystem. In VERA, the temperature enters in two ways: it partially determines the width of optical transitions by affecting the population of low frequency modes,[42] and it defines the detailed balance between the upward and downward IC and IVR rates. An elevated local temperature should therefore slow down net relaxation rates and alter spectral line shapes in a detectable way and may even give rise to the vibrational population inversion responsible for S*. The model assumed that energy lost from the vibronic subsystem during IC/IVR instantly equilibrated across all vibrational modes of the carotenoid. A temperature can be assigned to this pseudoequilibrium according to

$$\varepsilon(T) = \sum_n^N \frac{\hbar\omega_n}{2} \left(\frac{\exp\left(\frac{\hbar\omega_n}{k_B T} \right) + 1}{\exp\left(\frac{\hbar\omega_n}{k_B T} \right) - 1} \right) \quad (15)$$

https://doi.org/10.1021/acs.jpcb.2c00996
J. Phys. Chem. B 2022, 126, 3985−3994

where ω_n is the frequency of the nth vibrational normal mode (out of a total of N) which can be estimated from quantum chemical calculations on the ground state. We can now interpolate a local temperature via

$$\varepsilon(T_{loc}, t) = \varepsilon(T_\infty) + (\varepsilon_{pump} - \varepsilon_{i,a}(t)) \tag{16}$$

where ε_{pump} is the total energy that was delivered by the pump pulse, $\varepsilon_{i,a}(t)$ is the total energy currently in the vibronic subsystem, and T_∞ is the temperature of the bulk solvent. Energy transfer from the carotenoid to the FSS and then to the bulk is modeled as thermal diffusion:

$$\frac{\mathrm{d}}{\mathrm{d}t}T_{loc} = \delta T_{loc}(t) - N_S\gamma\frac{c_S}{c}(T_{loc} - T_{FSS}) \tag{17}$$

$$\frac{\mathrm{d}}{\mathrm{d}t}T_{FSS} = \gamma(T_{loc} - T_{FSS}) - \frac{3\chi}{R_{FSS}{}^2}(T_{FSS} - T_\infty) \tag{18}$$

Here $\delta T_{loc}(t)$ represents the incoming energy (from IC and IVR). Heat is lost to the FSS, which contains N_S molecules and has heat capacity c_S. γ is a solvent−solute coupling strength, and c is the heat capacity of the carotenoid. Heat transfer from the FSS to the bulk depends on the solvent diffusivity, χ, and the radius of the FSS, R_{FSS}. While χ, c_S, and c are simple chemical parameters, N_S, γ, and R_{FSS} are not, but can be estimated from, as in ref 24, molecular dynamics simulations. This model was applied to canthaxanthin and rhodoxanthin. Both pigments exhibit S* signals that decay slower than S_1, significantly so for rhodoxanthin, whose S_1 and S* lifetimes are 1.1 and 5.6 ps, respectively.[17] Rhodoxanthin also exhibits unusual positive signals in the region of the GSB at long times that are difficult to explain with standard VERA. If one were to convert all energy delivered by the pump into a local molecular temperature, one gets a theoretical maximum of $(T_{loc})_{max} \sim 550$ K. However, this is never reached since IC and IVR compete with cooling of the molecule and the FSS. Even if it were, it is insufficient to significantly slow the rate of IVR to generate a significant transient thermal population on the high frequency, optically coupled modes. This means that S* really does seem to arise from an *intrinsically slow* vibrational relaxation on S_0 and further work is needed to establish why this is the case and why it is so solvent dependent. Local heating does however explain the GSB distortions in the TA of rhodoxanthin, which arises from transient thermal broadening of linear absorption relative to the steady state absorption. These are the first hints that low-frequency vibrational dynamics and nontrivial solute−solvent interactions may need to be carefully considered in further work.

VERA: LIMITATIONS AND POSSIBLE SOLUTIONS

Despite its successes, VERA suffers from a number of weaknesses. First, one can question the validity of the displaced oscillator model, particularly in the case of S_1. There is significant evidence that $S_1 \rightarrow S_0$ IC occurs through a conical intersection along a coordinate related to the C=C stretch.[5] This is probably related to the significant frequency upshift ($1520 \rightarrow 1750$ cm^{-1}) in that same mode on the S_1 state.[44,45] Even within the harmonic approximation, frequency differences between equivalent modes on different electronic levels will affect the rates of IVR and, through the nuclear overlaps $F^{\alpha}_{i\omega j\omega}$, IC. This is a relatively straightforward modification and should be the next improvement made. Accounting for anharmonicities and intersections will be much more challenging. This connects to the second limitation of overparametrization. The fact that close fits are obtained without considering anharmonicity and mode mixing is likely due to an overdetermined model. While we can be confident in the parameters associated with the S_1-S_n and S_0-S_2 line shapes, the dynamic parameters (particularly for S_2-S_1 relaxation) are harder to fit. Adding further detail to VERA will come at the cost of adding yet more fit parameters possibly to the point where it becomes of limited practical use. A way to mitigate this is with simultaneous fits to larger data sets. Independent TA experiment with NIR probing will define the S_1-S_2 displacements, while TA after direct two-photon excitation (2PE) of S_1 (see below) will be an alternative approach to probing the S_1 surface. Revisiting of transient grating measurements may also give a better picture of the S_2-S_1 relaxation step which can also be difficult to fit.[39,46]

A further limitation is posed by the fact that the IC and IVR rates are expressed in terms of *ad hoc* bath parameters—i.e., reorganization energies and damping frequencies−which are very difficult to relate to solute/solvent properties, which complicated further developments of the model. For example, we term vibrational relaxation "IVR" because physically it is (mostly) the redistribution of vibrational energy from the optical modes to other uncoupled vibrations. This is mediated by the anharmonic resonances and cooperativities between neighboring modes which in turn are strongly affected by solvent interactions. Currently, VERA does not consider the dynamics of IVR. It merely keeps track of the energy exiting the vibronic subsystem and then portions it out to the low frequency modes. The rate at which this happens is still determined by the bath parameters. Incorporating a more realistic description of IVR into VERA will be a considerable challenge and will require extensive parametrization via quantum chemical calculations and measurements probing low-frequency vibrational dynamics. This becomes particularly tricky when we consider excited states where IVR overlaps with complex IC processes as shown below.

PERSPECTIVE: VERA ON TWO-PHOTON INITIATED ULTRAFAST DYNAMICS

A brand-new challenge for the theoretical approaches was set by the femtosecond time-resolved two-photon excitation (2PE) experiments.[47−50] Due to its multielectron character, the S_0-S_1 transition is one-photon forbidden, but two-photon allowed. Considering that two-photon excitation does not populate the S_2, the 2PE transient absorption spectra can be viewed as the "pure" S_1 state, minimizing artifacts arising from the depopulation of the higher lying energy levels. Due to the relatively low two-photon cross section of carotenoids, a large photon flux of $10^{16}-10^{17}$ photons/cm^2 per pulse has to be applied. This also affects the solvation shell: First, there is more heat in the solvation shell compared to one-photon excitation. Second, the solvent itself can be excited since most of the solvents have absorption peaks in the NIR region. These facts have to be considered in the theoretical calculation, because they clearly influence the experimental results. This is shown in Figure 2a, showing 2PE data which have not been reported previously. The transient absorption data of lutein in acetone after 2PE at 1210, 1250, and 1300 nm are shown at the delay time 1.4 ps. (The transient absorption spectra at earlier times are contaminated by the strong coherent artifact.) The experimental setup for 2PE transient absorption spectroscopy was described in detail previously.[48] Briefly, a Spitfire Ace regenerative amplifier system (Spectra Physics), seeded with a Ti:sapphire oscillator (MaiTai SP, Spectra Physics) and pumped by a Nd:YLF laser (Empower 30, Spectra Physics), was used for

https://doi.org/10.1021/acs.jpcb.2c00996
J. Phys. Chem. B 2022, 126, 3985−3994

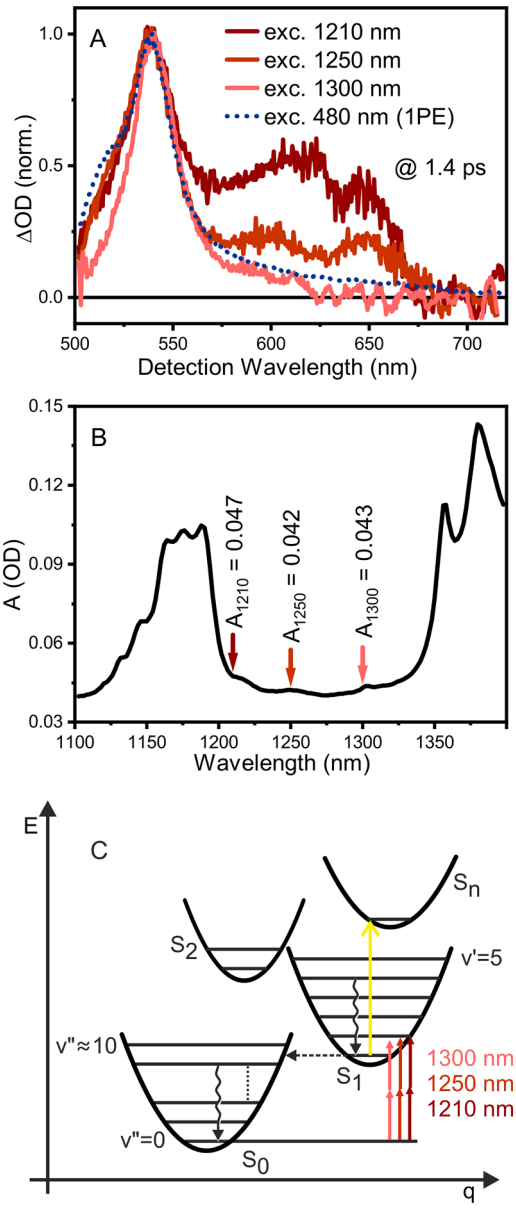

Figure 2. (A) Transient absorption spectra of lutein in acetone at 1.4 ps after 1210, 1250, and 1300 nm (shades of red) two-photon excitation. Transient absorption spectrum obtained after one photon excitation of the S_2 state at 480 nm is shown for comparison. (B) Steady state absorption spectrum of acetone in the NIR spectral region. Arrows represent two-photon energies used to excite the samples in the 2PE experiment and the corresponding absorbance in 2 mm cuvette, used for the experiments. (C) Energy level scheme describing electronic (dashed horizontal lines) and vibrational (wavy vertical lines) energy relaxation in lutein along reaction coordinate q after two-photon (reddish arrows) excitation. Colored vertical arrows indicate allowed two-photon transitions.

generating excitation (pump) and probe pulses. The two-photon excitation wavelengths were achieved through parametric amplification (TOPAS Prime, Light Conversion). The pump intensity was set to ~3.5×10^{16} photons/pulse cm^2. The white-light supercontinuum (WLC) was generated by focusing a fraction of the 800 nm beam from the Spitfire Ace in a 2 mm sapphire plate. The polarization between pump and probe beams was set parallel by a $\lambda/2$ waveplate. Lutein was purchased from Sigma-Aldrich and dissolved in acetone to yield OD of 1.5 at 447 nm in a 2 mm quartz cuvette. The transient absorption measurements were made at room temperature, and the sample was mixed continuously with a stirrer. To check for possible photodegradation, steady-state absorption spectra were recorded before and after measurements.

All three spectra in Figure 2a exhibit the spectral features typical for carotenoids in the S_1 state. The distinct peak at 540 nm is assigned to the S_1-S_n transition, while its blue shoulder is identified as the S* state. The S* state is more pronounced for the excitation wavelengths with higher photon frequency. The transient absorption spectra after 1210 and 1250 nm excitation also contain additional signal in the spectral region between 575 and 675 nm.

The NIR steady state absorption spectrum of acetone is shown in Figure 2b. The arrows indicate the excitation wavelengths used in the 2PE experiments, and the values show the corresponding absorbance in 2 mm cuvette, used in the experiment. The excitation wavelengths were chosen according to the two criteria: (i) To make the 1PE of the solvent as low as possible (nonetheless, there exists a small difference in the solvent absorption at a given excitation wavelengths, which can be important, considering the pump excitation intensity needed for 2PE of carotenoid); (ii) To excite the S_1 state to the lowest vibrational energy levels. This is also shown in the energy level scheme in Figure 2c. Two-photon excitation (arrows in shades of red) populates the first and second vibrational energy level of the carotenoid. In contrast, by one-photon excitation of S_2 and subsequent depopulation to S_1 state as depicted in Figure 1a, approximately the fifth vibrational level of the S_1 state is reached, to relax to lower levels by internal vibrational relaxation.

A four-state implementation of VERA including (S_0, S_1, S_2, S_n) is not able to explain the feature at 575−675 nm for 2PE at 1210 nm excitation wavelength. To illustrate this, we first fit standard 1PE measurements of lutein in the same solvent, with the results shown in Figure 3a. The fit is very good apart from an inability to reproduce the enhanced S_1 shoulder at 525 nm at early times. It is possible to capture this but only at the expense of the fit to the long wavelength (>550 nm) tail which here is the region of interest. This discrepancy may be the result of some of the limitations of VERA discussed above. The fits at earlier times are similar and not shown purely for clarity. Using these parameters, we then tried to fit the 2PE data. For 1300 nm excitation the fit is reasonable (not shown) and looks identical with the main S_1 peak in the 1PE data in Figure 3a and the 1210 nm TPE data in Figure 3b. To fit the main S_1 peak in the 1210 nm excitation data, however, it was necessary to decrease (relative to the values we obtained by fitting the 1PE data) the reorganization energies associated with vibrational relaxation on S_1, λ_α^1, by a factor of approximately $^1/_2$. This may be meaningful or simply reflect the fact that vibrational relaxation on S_1 is harder to unambiguously resolve in the 1PE kinetics. The model clearly fails to reproduce the feature at 575−675 nm. If we assume that this is some vibronic feature on S_1 (1210 nm should excite $|1_{20}\rangle$ or $|1_{11}\rangle$) then the question is why it relaxes so slowly. One possibility (see below) is that at 1210 nm we are transiently heating the solvent. The dotted red line in Figure 3b shows the relaxation kinetics with T = 10 000 K (purely to exaggerate any effects). We see that heating does produce a vibronic feature on the red edge of S_1, although it is neither broad enough nor in the correct position. Moreover, at reasonable temperatures, these effects are very small. Lastly, the dotted brown line in Figure 3b we simply set λ_α^1 = 0 and find that it produces red and blue vibronic shoulders and significantly slows down the S_1 relaxation kinetics. This clearly

https://doi.org/10.1021/acs.jpcb.2c00996
J. Phys. Chem. B 2022, 126, 3985−3994

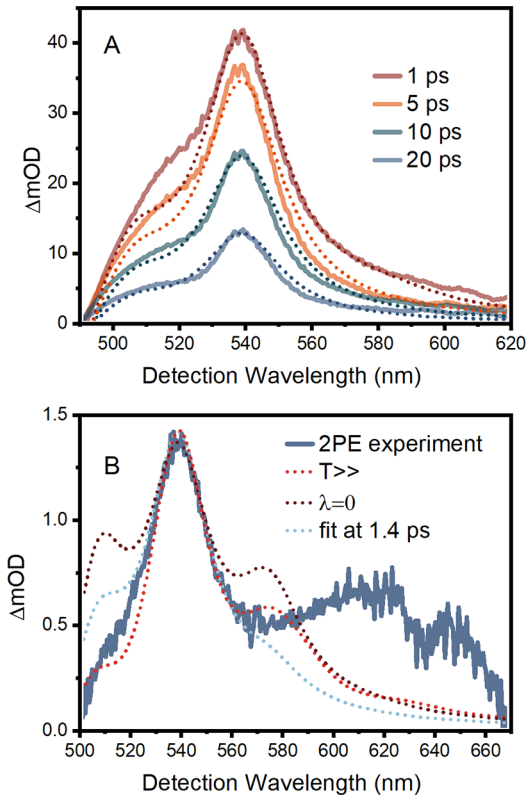

Figure 3. (A) Evolution of the experimental transient absorption signal of lutein in acetone in the S_1 ESA region of lutein in acetone following one-photon excitation of S_2 (solid lines). The fits obtained from VERA are shown as dotted lines, where we note the failure to fit the enhanced shoulder on blue edge of S_1 at early times. (B) Experimental transient absorption signal following direct, two-photon excitation of S_1 at 1210 nm (blue line). While VERA (with parameters taken from the one-photon fits except for λ_{ω}^{1}, which had to be reduced by a factor of approximately $^1/_2$) reproduces the main ESA peak reasonably well, it fails to reproduce the broad positive feature between 575 and 675 nm at early times. Raising the solvent temperature in the VERA model (here 10 000 K to exaggerate features) results in line-broadening and slowing of both internal conversion and vibrational relaxation (dotted red line). The vibronic peaks resulting from the latter do not align with the 575−675 nm feature. Reducing the reorganization energy associated with vibrational relaxation on S_1, λ_{ω}^{1}, to zero does enhance the vibronic features but again does not capture the 575−675 nm feature.

does not match the measured traces but even if it had, it would not tell us why vibrational relaxation rate was affected by the excitation wavelength. That is not to say that this feature at 575−675 nm is not the result of solvent excitation, merely that it is not a trivial heating effect. Similarly, it may also be a quirk of S_1 not captured by the simple displaced oscillator model.

Excitation Wavelength Dependent 2PE-Induced Dynamics. The inability to reliably fit the 2PE transient absorption data within the current VERA model provides important information about its limitation and sets directions to its improvement. This clearly shows that new experimental approaches are needed to fully understand the yet-unresolved issue related to the carotenoid S* state and its role in heat dissipation. While a lot of 1PE transient absorption data on various carotenoids is reported in the literature, there is still much space to expand 2PE transient absorption experiments. The 2PE data shown in Figure 2a are still limited to relatively narrow range of excitation wavelengths and even the lowest energy excitation at 1300 nm (7700 cm^{-1}) is approximately 1500 cm^{-1} above the expected vibrationless two-photon transition (0−0) of lutein.[51] Thus, shifting the 2PE wavelength to 1400 nm offers the possibility to excite the bottom of the S_1 potential surface, providing the least possible energy to excite lutein. On the other hand, 1400 nm will significantly excite the solvent via 1PE (Figure 2b), testing the hypothesis of direct solvent excitation as a source of the extra signal in Figure 2a. The NIR absorption of solvents (Figure 2b) has been largely ignored in spectroscopic experiments, yet it offers unique possibility to deposit some energy directly to the solvent. The NIR spectral bands are due to overtones and combinational vibrational bands,[52] thus tuning excitation to these bands does not promote the solvent to an electronic excited state but excites ground state vibrations instead. Of course, the same can be achieved by excitation of IR vibrational bands in the 800−3000 cm^{-1} (3.3−12.5 μm). Especially in time-resolved experiments, however, it is much easier to generate high-intensity tunable excitation in the NIR (1200−2500 nm) spectral region. Thus, time-resolved experiments using NIR excitation may cause a "local heating" of the solvent within the excitation spot, by depositing energy into ground state vibrations, effectively introducing a precisely timed temperature jump to the solvent. Such a temperature jump should be, in principle, detectable as it affects both the vibrational relaxation and internal conversion rates and alter line shapes (due to enhanced participation of low frequency vibrational modes of the carotenoid). In terms of the formalism described above, pre-excitation with a solvent-resonant NIR pulse lets us tune ε_{pump} in eq 16, in an effort to study temperature dependent effect of the energy flow between the carotenoid and the FSS. More generally, such a combined experimental-theoretical approach can help to pinpoint the response of the solute to the local heating of solvent.

PERSPECTIVE: NEW APPROACHES

In this final section, we want to outline future research directions based on the above concepts. Therefore, the selection below represents the personal opinions of the authors rather than possible trends in the entire research field of ultrafast carotenoid photophysics.

Temperature Dependent TA Measurements. As the heat dissipation/vibrational energy transfer is the central problem related to the VERA and its explanation of the S* signal in carotenoids, temperature-dependent experiments are of interest here. While data measured at cryogenic temperatures are available,[13] essentially no experiments were conducted at elevated temperatures. Except temperature-dependent absorption spectra of β-carotene suggesting that the S* might be related to the hot ground signal,[18] there are no transient absorption data taken at temperatures above room temperature. Here, problems with sample stability will certainly play a role, but preliminary experiments indicate that bulk heating to 50 °C should be readily achieved at least for some prototypical carotenoids.

Multipulse Experiments. As discussed in the model-section, VERA is successful in describing the vastly different time scales of S*-relaxation in carotenoids of varying chain length. The downside of this approach is the large number of model parameters, some of which have to be determined by multiparameter fitting. The reorganization energies of the fluctuations that induce IVR on S_0, λ_{ω}^{0}, are of particular interest here as VERA predicts relatively small values in order to reproduce the slow S*-relaxation times for long carotenoids. Hence, experimental verification of the retrieved values for λ_{α}^{0} in

https://doi.org/10.1021/acs.jpcb.2c00996
J. Phys. Chem. B 2022, 126, 3985−3994

multipulse experiments such as photon echo peak shift[53] or 2D electronic spectroscopy[54,55] and subsequent analysis would aid the validation of the results by VERA. Furthermore, our model predicts a large difference between reorganization energies on S_1 and S_0 for long-chain carotenoids. The former parameter, λ_α^1, calls for excited state parametrization as for example achieved in pump-degenerate four wave mixing[46,56] or FSRS.[15,57]

Application of VERA on Keto-carotenoids. Fucoxanthin and peridinin are prominent examples of carotenoids with carbonyl groups as part of the delocalized π-electron system. In polar solvents, initial excitation of S_2 may lead to energy transfer toward S_1 as well as toward an intramolecular charge transfer state (ICT). Zigmantas and co-workers[58] proposed a model with a common excited state, S_1/ICT, viewed as a double well potential with two minima for S_1 and ICT respectively, to explain temperature and solvent dependent TA-results. Such a double well with a pronounced vibrational level structure is an ideal scenario for VERA, where the interconversion between the S_1 and ICT minima is vibronically mediated. Such a study will contribute to the discussion whether the ICT or the S_1 state is the main energy donor toward chlorophylls in keto-carotenoid containing light harvesting systems.[59,60]

AUTHOR INFORMATION

Corresponding Author

Jürgen Hauer − *Dynamical Spectroscopy, Department of Chemistry, Technical University of Munich, 85748 Garching bei Munich, Germany;* orcid.org/0000-0002-6874-6138; Email: juergen.hauer@tum.de

Authors

Václav Šebelík − *Dynamical Spectroscopy, Department of Chemistry, Technical University of Munich, 85748 Garching bei Munich, Germany;* orcid.org/0000-0002-9597-3117

Christopher D. P. Duffy − *Digital Environment Research Institute, Queen Mary University of London, London E1 4NS, U.K.*

Erika Keil − *Dynamical Spectroscopy, Department of Chemistry, Technical University of Munich, 85748 Garching bei Munich, Germany*

Tomáš Polívka − *Department of Physics, Faculty of Science, University of South Bohemia, 370 05 České Budějovice, Czech Republic; Biology Centre, Institute of Plant Molecular Biology, Czech Academy of Sciences, 370 05 České Budějovice, Czech Republic;* orcid.org/0000-0002-6176-0420

Complete contact information is available at: https://pubs.acs.org/10.1021/acs.jpcb.2c00996

Author Contributions

$^{\perp}$V.S. and C.D.P.D. contributed equally. The manuscript was written through contributions of all authors. All authors have given approval to the final version of the manuscript.

Notes

The authors declare no competing financial interest.

Biographies

Václav Šebelík, Ph.D., is a postdoctoral researcher in the group of Prof. Dr. J. Hauer at the Technical University of Munich (TUM). He obtained his Ph.D. degree at the University of South Bohemia, where he was mainly focused on ultrafast spectroscopy of photosynthetic pigments and pigment−protein complexes. Here, he gained a great interest in the dark excited states of carotenoids and the methods allowing their direct excitation. Currently, he continues to investigate energy transfer processes in the light-harvesting complexes by means of the transient absorption spectroscopy.

Dr. Christopher D. P. Duffy is a theoretical physicist with research interests in fast energy relaxation processes in carotenoids and their roles in photosynthetic light-harvesting. He initially focused on the role of the optically forbidden S_1 state in the photoprotective non-photochemical quenching (NPQ) mechanism in higher plants. More recently he has become more generally interested in the complex role of solute−solvent interactions in the carotenoid relaxation, identifying the signatures of transient local superheating in their optical spectra.

Erika Keil is a doctoral candidate in Physical Chemistry at the Department of Chemistry at the Technical University of Munich (TUM). She graduated from TUM with a M.Sc. degree majoring in Physical and Theoretical Chemistry (2018−2021). She completed her master's thesis under the supervision of Prof. Dr. J. Hauer on ultrashort pulse generation in the blue-green spectral region by achromatic frequency doubling. In the summer of 2021, she enrolled in the graduate program at TUM and has since been advised by Prof. Dr. J. Hauer toward a dissertation focusing on ultrafast multidimensional spectroscopy in the blue-green spectral region, with the goal of gaining a deeper insight into the photophysics of light harvesting processes in diatoms. Her current research interests entail the bio- and photophysics of carotenoids, energy transfer processes in light harvesting complexes and multidimensional spectroscopy.

Tomáš Polívka is a professor of biophysics at the University of South Bohemia. He is a leader of ultrafast spectroscopy group, and his research is predominantly focused on ultrafast photophysics and photochemistry of carotenoids. His current research activities extend from roles of carotenoids in light harvesting and photoprotection in photosynthesis to studies of excess energy dissipation at a molecular level.

Jürgen Hauer is a physical chemist at TUM and head of the Dynamical Spectroscopies group. His interest in carotenoids and natural light harvesting dynamics in general was triggered during his Ph.D. work with Prof. Marcus Motzkus. Multidimensional spectroscopy methods such as two-dimensional electronic spectroscopy in both 3rd and 5th order variants are at the heart of his research interest, and he was and is applying such methods on carotenoids and photosynthetic systems.

ACKNOWLEDGMENTS

J.H. and V.S. acknowledge funding by the DFG under Germany's Excellence Strategy—EXC 2089/1-390776260. C.D.P.D. would like acknowledge support from the Biotechnology and Biological Sciences Research Council (BBSRC, Grant Number: BB/T000023/1). T.P. thanks the Czech Science Foundation (19-28323X) and the Ministry of Education, Youth and Sports of the Czech Republic with cofinancing from the EU (KOROLID, CZ.02.1.01/0.0/0.0/15_003/0000336).

REFERENCES

(1) Polívka, T.; Sundström, V. Ultrafast Dynamics of Carotenoid Excited States-From Solution to Natural and Artificial Systems. *Chem. Rev.* **2004**, *104*, 2021−2071.

(2) Staleva, H.; Zeeshan, M.; Chábera, P.; Partali, V.; Sliwka, H. R.; Polívka, T. Ultrafast Dynamics of Long Homologues of Carotenoid Zeaxanthin. *J. Phys. Chem. A* **2015**, *119*, 11304−11312.

(3) Andersson, P. O.; Gillbro, T. Photophysics and Dynamics of the Lowest Excited Singlet State in Long Substituted Polyenes with Implications to the Very Long-Chain Limit. *J. Chem. Phys.* **1995**, *103*, 2509−2519.

(4) Polívka, T.; Sundström, V. Dark Excited States of Carotenoids: Consensus and Controversy. *Chem. Phys. Lett.* **2009**, *477*, 1−11.

(5) Gradinaru, C. C.; Kennis, J. T. M.; Papagiannakis, E.; Van Stokkum, I. H. M.; Cogdell, R. J.; Fleming, G. R.; Niederman, R. A.; Van Grondelle, R. An Unusual Pathway of Excitation Energy Deactivation in Carotenoids: Singlet-to-Triplet Conversion on an Ultrafast Timescale in a Photosynthetic Antenna. *Proc. Natl. Acad. Sci. U. S. A.* **2001**, *98*, 2364−2369.
(6) Wohlleben, W.; Buckup, T.; Hashimoto, H.; Cogdell, R. J.; Herek, J. L.; Motzkus, M. Pump-Deplete-Probe Spectroscopy and the Puzzle of Carotenoid Dark States. *J. Phys. Chem. B* **2004**, *108*, 3320−3325.
(7) Frank, H. A.; Cua, A.; Chynwat, V.; Young, A.; Gosztola, D.; Wasielewski, M. R. Photophysics of the Carotenoids Associated with the Xanthophyll Cycle in Photosynthesis. *Photosynth. Res.* **1994**, *41*, 389−395.
(8) Jailaubekov, A. E.; Song, S. H.; Vengris, M.; Cogdell, R. J.; Larsen, D. S. Using Narrowband Excitation to Confirm That the S* State in Carotenoids Is Not a Vibrationally-Excited Ground State Species. *Chem. Phys. Lett.* **2010**, *487*, 101−107.
(9) Niedzwiedzki, D. M.; Sullivan, J. O.; Polívka, T.; Birge, R. R.; Frank, H. A. Femtosecond Time-Resolved Transient Absorption Spectroscopy of Xanthophylls. *J. Phys. Chem. B* **2006**, *110*, 22872−22885.
(10) Niedzwiedzki, D.; Koscielecki, J. F.; Cong, H.; Sullivan, J. O.; Gibson, G. N.; Birge, R. R.; Frank, H. A. Ultrafast Dynamics and Excited State Spectra of Open-Chain Carotenoids at Room and Low Temperatures. *J. Phys. Chem. B* **2007**, *111*, 5984−5998.
(11) Jailaubekov, A. E.; Vengris, M.; Song, S. H.; Kusumoto, T.; Hashimoto, H.; Larsen, D. S. Deconstructing the Excited-State Dynamics of β-Carotene in Solution. *J. Phys. Chem. A* **2011**, *115*, 3905−3916.
(12) Papagiannakis, E.; Van Stokkum, I. H. M.; Vengris, M.; Cogdell, R. J.; Van Grondelle, R.; Larsen, D. S. Excited-State Dynamics of Carotenoids in Light-Harvesting Complexes. 1. Exploring the Relationship between the S_1 and S* States. *J. Phys. Chem. B* **2006**, *110*, 5727−5736.
(13) Hauer, J.; Maiuri, M.; Viola, D.; Lukes, V.; Henry, S.; Carey, A. M.; Cogdell, R. J.; Cerullo, G.; Polli, D. Explaining the Temperature Dependence of Spirilloxanthin's S* Signal by an Inhomogeneous Ground State Model. *J. Phys. Chem. A* **2013**, *117*, 6303−6310.
(14) Lukeš, V.; Christensson, N.; Milota, F.; Kauffmann, H. F.; Hauer, J. Electronic Ground State Conformers of β-Carotene and Their Role in Ultrafast Spectroscopy. *Chem. Phys. Lett.* **2011**, *506*, 122−127.
(15) Kloz, M.; Weißenborn, J.; Polívka, T.; Frank, H. A.; Kennis, J. T. M. Spectral Watermarking in Femtosecond Stimulated Raman Spectroscopy: Resolving the Nature of the Carotenoid S* State. *Phys. Chem. Chem. Phys.* **2016**, *18*, 14619−14628.
(16) Papagiannakis, E.; Van Stokkum, I. H. M.; Van Grondelle, R.; Niederman, R. A.; Zigmantas, D.; Sundström, V.; Polívka, T. A Near-Infrared Transient Absorption Study of the Excited-State Dynamics of the Carotenoid Spirilloxanthin in Solution and in the LH1 Complex of *Rhodospirillum rubrum*. *J. Phys. Chem. B* **2003**, *107*, 11216−11223.
(17) Chábera, P.; Fuciman, M.; Hříbek, P.; Polívka, T. Effect of Carotenoid Structure on Excited-State Dynamics of Carbonyl Carotenoids. *Phys. Chem. Chem. Phys.* **2009**, *11*, 8795−8803.
(18) Lenzer, T.; Ehlers, F.; Scholz, M.; Oswald, R.; Oum, K. Assignment of Carotene S* State Features to the Vibrationally Hot Ground Electronic State. *Phys. Chem. Chem. Phys.* **2010**, *12*, 8832−8839.
(19) Lenzer, T.; Schubert, S.; Ehlers, F.; Lohse, P. W.; Scholz, M.; Oum, K. Femtosecond Pump-Supercontinuum Probe and Transient Lens Spectroscopy of Adonixanthin. *Arch. Biochem. Biophys.* **2009**, *483*, 213−218.
(20) Ehlers, F.; Scholz, M.; Oum, K.; Lenzer, T. Excited-State Dynamics of 3,3′-Dihydroxyisorenieratene and (3R,3′R)-Zeaxanthin: Observation of Vibrationally Hot S_0 Species. *Arch. Biochem. Biophys.* **2018**, *646*, 137−144.
(21) Ehlers, F.; Scholz, M.; Schimpfhauser, J.; Bienert, J.; Oum, K.; Lenzer, T. Collisional Relaxation of Apocarotenals: Identifying the S* State with Vibrationally Excited Molecules in the Ground Electronic State S_0*. *Phys. Chem. Chem. Phys.* **2015**, *17*, 10478−10488.
(22) Balevičius, V.; Pour, A. G.; Savolainen, J.; Lincoln, C. N.; Lukeš, V.; Riedle, E.; Valkunas, L.; Abramavicius, D.; Hauer, J. Vibronic Energy Relaxation Approach Highlighting Deactivation Pathways in Carotenoids. *Phys. Chem. Chem. Phys.* **2015**, *17*, 19491−19499.
(23) Balevičius, V.; Abramavicius, D.; Polívka, T.; Galestian Pour, A.; Hauer, J. A Unified Picture of S* in Carotenoids. *J. Phys. Chem. Lett.* **2016**, *7*, 3347−3352.
(24) Balevičius, V.; Wei, T.; Di Tommaso, D.; Abramavicius, D.; Hauer, J.; Polívka, T.; Duffy, C. D. P. The Full Dynamics of Energy Relaxation in Large Organic Molecules: From Photo-Excitation to Solvent Heating. *Chem. Sci.* **2019**, *10*, 4792−4804.
(25) Papagiannakis, E.; Kennis, J. T. M.; Van Stokkum, I. H. M.; Cogdell, R. J.; Van Grondelle, R. An Alternative Carotenoid-to-Bacteriochlorophyll Energy Transfer Pathway in Photosynthetic Light Harvesting. *Proc. Natl. Acad. Sci. U. S. A.* **2002**, *99*, 6017−6022.
(26) Gould, S. L.; Kodis, G.; Palacios, R. E.; De La Garza, L.; Brune, A.; Gust, D.; Moore, T. A.; Moore, A. L. Artificial Photosynthetic Reaction Centers with Porphyrins as Primary Electron Acceptors. *J. Phys. Chem. B* **2004**, *108*, 10566−10580.
(27) Liguori, N.; Xu, P.; Van Stokkum, I. H. M.; Van Oort, B.; Lu, Y.; Karcher, D.; Bock, R.; Croce, R. Different Carotenoid Conformations Have Distinct Functions in Light-Harvesting Regulation in Plants. *Nat. Commun.* **2017**, *8*, 1994.
(28) Saccon, F.; Durchan, M.; Bína, D.; Duffy, C. D. P.; Ruban, A. V.; Polívka, T. A Protein Environment-Modulated Energy Dissipation Channel in LHCII Antenna Complex. *iScience* **2020**, *23*, 101430.
(29) Mascoli, V.; Gelzinis, A.; Chmeliov, J.; Valkunas, L.; Croce, R. Light-Harvesting Complexes Access Analogue Emissive States in Different Environments. *Chem. Sci.* **2020**, *11*, 5697−5709.
(30) Konold, P. E.; Van Stokkum, I. H. M.; Muzzopappa, F.; Wilson, A.; Groot, M. L.; Kirilovsky, D.; Kennis, J. T. M. Photoactivation Mechanism, Timing of Protein Secondary Structure Dynamics and Carotenoid Translocation in the Orange Carotenoid Protein. *J. Am. Chem. Soc.* **2019**, *141*, 520−530.
(31) Niedzwiedzki, D. M.; Hunter, C. N.; Blankenship, R. E. Evaluating the Nature of So-Called S*-State Feature in Transient Absorption of Carotenoids in Light-Harvesting Complex 2 (LH2) from Purple Photosynthetic Bacteria. *J. Phys. Chem. B* **2016**, *120*, 11123−11131.
(32) Tavan, P.; Schulten, K. Electronic Excitations in Finite and Infinite Polyenes. *Phys. Rev. B* **1987**, *36*, 4337−4358.
(33) Pendon, Z. D.; Sullivan, J. O.; Van Der Hoef, I.; Lugtenburg, J.; Cua, A.; Bocian, D. F.; Birge, R. R.; Frank, H. A. Stereoisomers of Carotenoids: Spectroscopic Properties of Locked and Unlocked Cis-Isomers of Spheroidene. *Photosynth. Res.* **2005**, *86*, 5−24.
(34) Macernis, M.; Sulskus, J.; Duffy, C. D. P.; Ruban, A. V.; Valkunas, L. Electronic Spectra of Structurally Deformed Lutein. *J. Phys. Chem. A* **2012**, *116*, 9843−9853.
(35) Kleinschmidt, M.; Marian, C. M.; Waletzke, M.; Grimme, S. Parallel Multireference Configuration Interaction Calculations on Mini-β-Carotenes and β-Carotene. *J. Chem. Phys.* **2009**, *130*, 044708.
(36) Greco, J. A.; LaFountain, A. M.; Kinashi, N.; Shinada, T.; Sakaguchi, K.; Katsumura, S.; Magdaong, N. C. M.; Niedzwiedzki, D. M.; Birge, R. R.; Frank, H. A. Spectroscopic Investigation of the Carotenoid Deoxyperidinin: Direct Observation of the Forbidden $S_0 \rightarrow S_1$ Transition. *J. Phys. Chem. B* **2016**, *120*, 2731−2744.
(37) Bondanza, M.; Jacquemin, D.; Mennucci, B. Excited States of Xanthophylls Revisited: Toward the Simulation of Biologically Relevant Systems. *J. Phys. Chem. Lett.* **2021**, *12*, 6604−6612.
(38) Kurashige, Y.; Nakano, H.; Nakao, Y.; Hirao, K. The $\pi \rightarrow \pi^*$ Excited States of Long Linear Polyenes Studied by the CASCI-MRMP Method. *Chem. Phys. Lett.* **2004**, *400*, 425−429.
(39) Sugisaki, M.; Yanagi, K.; Cogdell, R. J.; Hashimoto, H. Unified Explanation for Linear and Nonlinear Optical Responses in β-Carotene: A Sub-20-Fs Degenerate Four-Wave Mixing Spectroscopic Study. *Phys. Rev. B - Condens. Matter Mater. Phys.* **2007**, *75*, 155110.
(40) Sugisaki, M.; Fujiwara, M.; Yanagi, K.; Cogdell, R. J.; Hashimoto, H. Four-Wave Mixing Signals from β-Carotene and Its n = 15 Homologue. *Photosynth. Res.* **2008**, *95*, 299−308.

https://doi.org/10.1021/acs.jpcb.2c00996
J. Phys. Chem. B 2022, 126, 3985−3994

(41) Sugisaki, M.; Fujiwara, M.; Nair, S. V.; Ruda, H. E.; Cogdell, R. J.; Hashimoto, H. Excitation-Energy Dependence of Transient Grating Spectroscopy in β-Carotene. *Phys. Rev. B - Condens. Matter Mater. Phys.* **2009**, *80*, 035118.
(42) Braem, O.; Penfold, T. J.; Cannizzo, A.; Chergui, M. A Femtosecond Fluorescence Study of Vibrational Relaxation and Cooling Dynamics of UV Dyes. *Phys. Chem. Chem. Phys.* **2012**, *14*, 3513−3519.
(43) Balevičius, V.; Lincoln, C. N.; Viola, D.; Cerullo, G.; Hauer, J.; Abramavicius, D. Effects of Tunable Excitation in Carotenoids Explained by the Vibrational Energy Relaxation Approach. *Photosynth. Res.* **2018**, *135*, 55−64.
(44) Hashimoto, H.; Uragami, C.; Yukihira, N.; Gardiner, A. T.; Cogdell, R. J. Understanding/Unravelling Carotenoid Excited Singlet States. *J. R. Soc. Interface* **2018**, *15*, 20180026.
(45) Hashimoto, H.; Koyama, Y. The C═C Stretching Raman Lines of β-Carotene Isomers in the S_1 State as Detected by Pump-Probe Resonance Raman Spectroscopy. *Chem. Phys. Lett.* **1989**, *154*, 321−325.
(46) Hauer, J.; Buckup, T.; Motzkus, M. Pump-Degenerate Four Wave Mixing as a Technique for Analyzing Structural and Electronic Evolution: Multidimensional Time-Resolved Dynamics near a Conical Intersection. *J. Phys. Chem. A* **2007**, *111*, 10517−10529.
(47) Kosumi, D.; Kusumoto, T.; Fujii, R.; Sugisaki, M.; Iinuma, Y.; Oka, N.; Takaesu, Y.; Taira, T.; Iha, M.; Frank, H. A.; Hashimoto, H. One- and Two-Photon Pump-Probe Optical Spectroscopic Measurements Reveal the S_1 and Intramolecular Charge Transfer States Are Distinct in Fucoxanthin. *Chem. Phys. Lett.* **2009**, *483*, 95−100.
(48) Šebelík, V.; Fuciman, M.; West, R. G.; Polívka, T. Time-Resolved Two-Photon Spectroscopy of Carotenoids. *Chem. Phys.* **2019**, *522*, 171−177.
(49) Šebelík, V.; Kuznetsova, V.; Lokstein, H.; Polívka, T. Transient Absorption of Chlorophylls and Carotenoids after Two-Photon Excitation of LHCII. *J. Phys. Chem. Lett.* **2021**, *12*, 3176−3181.
(50) Wehling, A.; Walla, P. J. A Two-Photon Excitation Study on the Role of Carotenoid Dark States in the Regulation of Plant Photosynthesis. *Photosynth. Res.* **2006**, *90*, 101−110.
(51) Niedzwiedzki, D. M.; Enriquez, M. M.; LaFountain, A. M.; Frank, H. A. Ultrafast Time-Resolved Absorption Spectroscopy of Geometric Isomers of Xanthophylls. *Chem. Phys.* **2010**, *373*, 80−89.
(52) Weyer, L. G. Near-Infrared Spectroscopy of Organic Substances. *Appl. Spectrosc. Rev.* **1985**, *21*, 1−43.
(53) Yang, M.; Fleming, G. R. Third-Order Nonlinear Optical Response and Energy Transfer in Static Disordered Systems. *J. Chem. Phys.* **2000**, *113*, 2823−2840.
(54) Christensson, N.; Milota, F.; Nemeth, A.; Sperling, J.; Kauffmann, H. F.; Pullerits, T.; Hauer, J. Two-Dimensional Electronic Spectroscopy of β-Carotene. *J. Phys. Chem. B* **2009**, *113*, 16409−16419.
(55) Calhoun, T. R.; Davis, J. A.; Graham, M. W.; Fleming, G. R. The Separation of Overlapping Transitions in β-Carotene with Broadband 2D Electronic Spectroscopy. *Chem. Phys. Lett.* **2012**, *523*, 1−5.
(56) Miki, T.; Buckup, T.; Krause, M. S.; Southall, J.; Cogdell, R. J.; Motzkus, M. Vibronic Coupling in the Excited-States of Carotenoids. *Phys. Chem. Chem. Phys.* **2016**, *18*, 11443−11453.
(57) Kukura, P.; McCamant, D. W.; Davis, P. H.; Mathies, R. A. Vibrational Structure of the S_2 ($1B_u$) Excited State of Diphenyloctatetraene Observed by Femtosecond Stimulated Raman Spectroscopy. *Chem. Phys. Lett.* **2003**, *382*, 81−86.
(58) Zigmantas, D.; Polívka, T.; Hiller, R. G.; Yartsev, A.; Sundström, V. Spectroscopic and Dynamic Properties of the Peridinin Lowest Singlet Excited States. *J. Phys. Chem. A* **2001**, *105*, 10296−10306.
(59) West, R. G.; Bína, D.; Fuciman, M.; Kuznetsova, V.; Litvín, R.; Polívka, T. Ultrafast Multi-Pulse Transient Absorption Spectroscopy of Fucoxanthin Chlorophyll a Protein from *Phaeodactylum tricornutum*. *Biochim. Biophys. Acta - Bioenerg.* **2018**, *1859*, 357−365.
(60) Redeckas, K.; Voiciuk, V.; Zigmantas, D.; Hiller, R. G.; Vengris, M. Unveiling the Excited State Energy Transfer Pathways in Peridinin-Chlorophyll a-Protein by Ultrafast Multi-Pulse Transient Absorption Spectroscopy. *Biochim. Biophys. Acta - Bioenerg.* **2017**, *1858*, 297−307.

https://doi.org/10.1021/acs.jpcb.2c00996
J. Phys. Chem. B 2022, 126, 3985−3994